Accepted Manuscript

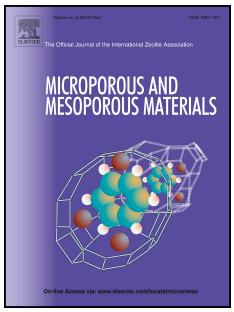

Decoding gas-solid interaction effects on adsorption isotherm shape: II. Polar adsorptives

S. Hadi Madani, Mark J. Biggs, Francisco Rodríguez-Reinoso, Phillip Pendleton

PII: S1387-1811(18)30618-8

DOI: https://doi.org/10.1016/j.micromeso.2018.11.039

Reference: MICMAT 9215

To appear in: *Microporous and Mesoporous Materials*

Received Date: 11 January 2018

Revised Date: 18 November 2018

Accepted Date: 28 November 2018

Please cite this article as: S.H. Madani, M.J. Biggs, F. Rodríguez-Reinoso, P. Pendleton, Decoding gas-solid interaction effects on adsorption isotherm shape: II. Polar adsorptives, *Microporous and Mesoporous Materials* (2018), doi: https://doi.org/10.1016/j.micromeso.2018.11.039.

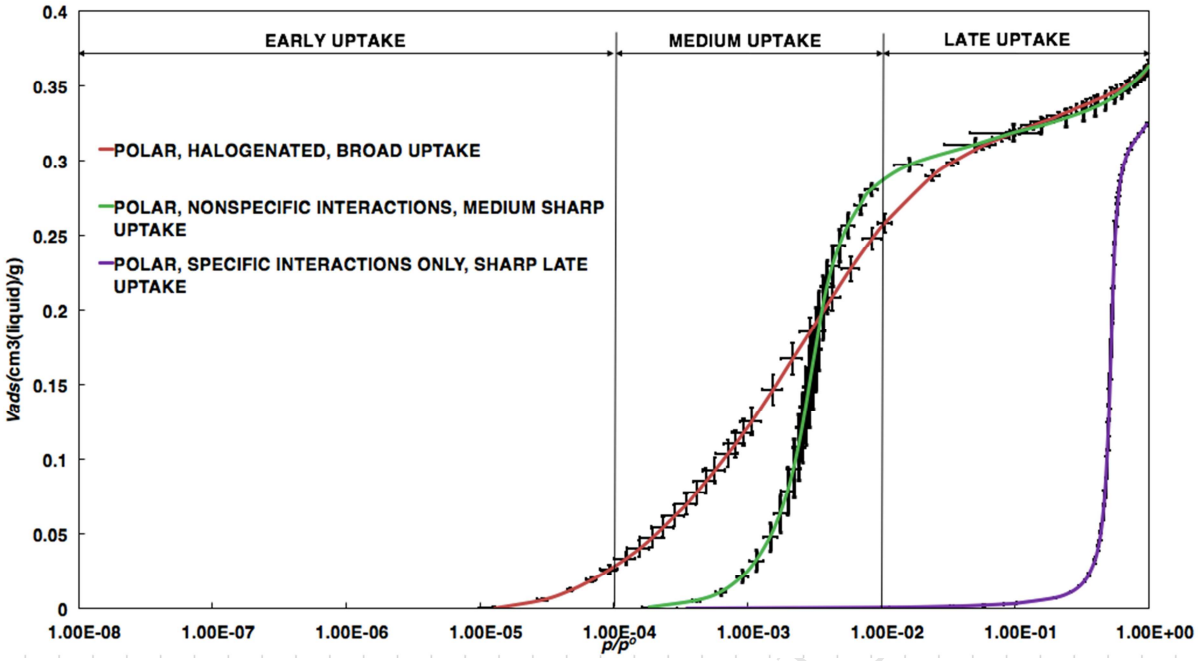

Decoding gas-solid interaction effects on adsorption isotherm shape: II. Polar adsorptives

S. Hadi Madani[a,b], *Mark J. Biggs*[c,*], *Francisco Rodríguez-Reinoso*[d], *Phillip Pendleton*[c,#]

[a] *Ian Wark Research Institute, University of South Australia, Adelaide, SA 5001, Australia*

[b] *Australian School of Petroleum, The University of Adelaide, Adelaide, SA 5005, Australia*

[c] *School of Chemical Engineering, The University of Adelaide, Adelaide, SA 5005, Australia.*

[d] *Laboratorio de Materiales Avanzados, Departamento de Química Inorgánica, Universidad de Alicante. Apartado 99; E-03080, Spain.*

[*] Current address: School of Science, Loughborough University, Leicestershire, LE11 3TU, UK

[#] Corresponding Author: E-mail: Phillip.Pendleton@adelaide.edu.au; Tel: +61 (0)8 8313 1265

KEYWORDS: adsorption**,** specific interaction, adsorbate, adsorbent, mechanism, polarity, polarizability

ABSTRACT

A unique set of 6 polar adsorptives of relatively large dipole moment and of increasing kinetic diameter were used to probe pore volumes available and their mechanism of adsorption on a well-characterized microporous carbon. Multiple adsorption isotherm measurements were made and repeatable results with relatively small standard deviations in amount adsorbed at low relative pressures were obtained. Inconsistencies were observed between calculated Gurvitsch volumes. Sources of these were analysed and identified as contributions from one or more of: (a) molecular sieve effects; (b) molecular packing effects, and; (c) 2D molecular structure formation due to hydrogen bonding. These inconsistencies were further studied by comparison with pore volumes derived *via* the Dubinin-Radushkevich (DR) equation. Qualitative analyses of the micropore filling processes were proposed, and substantiated by complementary DR analyses. Although most of the isotherms showed Type I character, recasting the relative pressure axis in logarithmic format highlighted clear differences as contributions from fluid-fluid and fluid-solid interactions during pore filling. Overall, the adsorptives were classified into three groups: (a) polar adsorptives with primarily specific interactions adsorbing as a condensation process over a relatively narrow relative pressure range in a medium and late pressure range (*iso*-PrOH, MeOH, 2-methyl, 2-butanol, H_2O); (b) polar adsorptives with potential for non-specific interactions adsorbing as a condensation process over a relatively narrow pressure range in a medium pressure range (pyridine, *iso*-PrOH, 2-methyl, 2-butanol); and, (c) halogenated adsorptives adsorbing with an S-shaped uptake extending over a broad relative pressure (dichloromethane).

INTRODUCTION

Nitrogen gas adsorption-based characterisation of porous materials is ubiquitous. Analysis of the obtained data produces information including adsorbent pore volume, pore size distribution (PSD) and, in some cases pore connectivity [1]. Porous adsorbent internal and external surface functional group type and their distribution across these surfaces might be defined via adsorption isotherm analyses of molecules of known shape, size, and adsorbed phase configuration. Such analyses are considerably less frequently applied than nitrogen or argon adsorption isotherm analyses. This contribution addresses an omission in the previously published literature, adsorption and analysis of a suite of polar molecules of similar dipole moment but different kinetic diameters adsorbed by a well-characterised activated carbon. A detailed analysis and interpretation of such a potentially unique collection of adsorption isotherms would provide greater insight into adsorptive polarity as well as size effects on micropore filling mechanisms.

Based on their polarity and their potential for specific interactions, adsorptives have been broadly classified as either non-polar or polar. The former offer non-specific or dispersion force-dominated interaction potentials employed in adsorption isotherm modelling. Typical adsorptives would be N_2, Ar, CO_2, SF_6, and C_6H_6. Adsorption of these by the carbon used in the current work has been discussed in detail [2]. The latter class exhibit specific interactions with either polar or polarizable surface groups. Typical adsorptives would be H_2O, alcohols, and amines, and others offering permanent dipole properties.

Since water-water intermolecular interaction energy tends to exceed water-carbon surface interaction energy [3], a generally accepted protocol for its adsorption with carbon adsorbents is an initial specific interaction with accessible surface polar or polarizable groups, followed by water cluster formation and, at sufficiently high vapour pressures, condensation within pores or across the non-porous surface [4-6]. Generally, pore filling occurs prior to non-porous surface condensation. Low pressure amounts adsorbed, interpreted as specific interactions, combined with specific surface area details usually derived from nitrogen or argon gas adsorption isotherm analyses lead to polar group surface-distribution details. These details are usually quoted as the number of functional groups or polarizable sites per unit area of surface [7, 8]. Such interpretation is equivocal for microporous adsorbents.

Although an analysis of the surface chemistry and its distribution on a well-characterised carbon adsorbent of well-defined PSD is lacking in the previously published literature, several contributions exist providing details from which surface chemistry influences on adsorption have been deduced. Bandosz and co-workers [9-11] compared multiple temperature adsorption isotherm results for H_2O and MeOH contacting similarly derived activated carbons with varying adjustments to adsorbent porosity and surface chemistry. For these, they concluded that while MeOH was susceptible to both

pore and surface chemistry changes, water adsorption was primarily affected by adsorbent surface chemistry. Separately, specific and non-specific interactions of H_2O, MeOH, and EtOH with activated carbons of different origins, containing dissimilar molar amounts of surface oxygen (per gram activated carbon), were assessed via adsorption and enthalpy of immersion measurements, using benzene as a reference vapour and liquid [12]. In this case, water adsorption and immersion enthalpy results were more responsive, increasing in amount adsorbed and exothermicity with increasing oxygen content. MeOH and EtOH showed smaller but similar trends, with MeOH exceeding EtOH for all measurements. These comparisons were made following the concepts underpinning the Theory for Volume Filling of Micropores (TVFM) [13-15]. The effects of adsorbent porosity on alcohol adsorption were removed in the work of Andreu *et al*.[16]. Their comparisons between MeOH, EtOH, and *iso*-PrOH adsorption and heat of immersion by variously increasing oxygen content on a non-porous carbon black surface demonstrated larger amounts of MeOH adsorbed with increasing oxygen content, but less marked effects for EtOH and *iso*-PrOH, interpreted as due to increasing contributions from dispersion force ethyl and propyl group interactions.

Bradley and Rand used N_2, MeOH, EtOH, *iso*-PrOH, *iso*-BuOH, Freon 113, and H_2O to characterize coal-, nutshell- and poly(vinylidene chloride)-based activated carbons [17]. They evaluated micropore volumes using Dubinin-Raduskevich model analyses of the N_2 adsorption isotherms. Isotherm interpretation for the larger adsorptives centred on molecular packing effects within the micropores, concluding a correction factor would be required using these to establish (nitrogen equivalent) micropore volumes. Interestingly, their application of the Dubinin-Serpinsky (D-S) model to analyse water adsorption and the effects of increasing surface polarity, concluded no unequivocal relationship existed between the number of primary adsorption sites and the parameter a_0 in the D-S model, which was defined as the specific amount of water adsorbed.

Rodriguez-Reinoso *et al.* attempted to distinguish non-specific adsorption due to microporosity from specific adsorption due to oxygen-based surface functional groups via analyses of N_2, SO_2, H_2O, and MeOH adsorption isotherms defined on variously oxidised, peach stone-based activated carbons [18]. By contrasting H_2O adsorption against MeOH adsorption they concluded that H_2O adsorbed specifically at relative pressures < 0.3, with condensation within micropores following at higher relative pressures; microporosity promoted MeOH adsorption at considerably lower relative pressures. Comparing each adsorptive, they found low relative pressure values on specific adsorbate-adsorbent interactions increased as $N_2 < SO_2 < CH_3OH < H_2O$, the differences being attributed to influences of adsorptive intermolecular (fluid-fluid) interactions due to the permanent polar moment (N_2 = 0, SO_2 = 1.6 D, CH_3OH = 1.7 D, H_2O = 1.8 D) and contributions from intermolecular hydrogen bonds. Immersion enthalpy into benzene for olive stone-based activated carbons, oxidised then reduced, showed independence of the extent of surface oxidation [19]. Immersion enthalpy of the same adsorbents into H_2O and MeOH, normalised to the benzene results, distinguished those surface groups

as CO-evolving groups (during heat treatment and reduction) more influential on the evolution of the enthalpy of immersion than CO_2-evolving groups.

The excluded volume manifests itself from either of the following criteria [2]:

1- *Molecular sieving effect*;

2- *Molecular packing effects governed by a critical ratio of pore size-to-probe size* [20];

3- *Molecular packing effects dictated by long-range structure development within the densified adsorbed volume*.

In this contribution, we build upon these foundational investigations by comparing and contrasting the isotherm shapes and location of condensation relative pressures in repeatedly measured, high-resolution adsorption isotherms of 6 polar vapours on a well-characterised, polymer-based, microporous activated carbon [7, 21-23]. As a set, the adsorptives exhibit a relatively large but moderately narrow-ranged dipole moment (1.85 ± 0.17 D), a wide range of kinetic diameters (0.41 ± 0.12 nm), and different molecular shapes. For each adsorptive, a Gurvitsch volume is estimated and compared with pore volumes derived via DR modelling, with the differences discussed in terms of pore filling and chemical and physical property effects on the gas-solid interactions. Isotherms are also presented in log-scale relative pressure where the isotherm shape is analysed to clarify specific adsorption and pore filling mechanisms. The pore filling mechanism is further explored and discussed in terms of DR plots. These analyses result in classifications of the adsorption isotherms based on the adsorptive likelihood for specific and/or non-specific interactions. We conclude that the methodologies and analyses developed and used here can be generalized to any adsorptive and, from this point of view, our presentation significantly extends and enhances the currently available literature.

MATERIALS AND METHODS

A well-characterised, poly(furfuryl alcohol)-based, activated carbon was used in this study as an exemplar microporous adsorbent. Its synthesis and activation procedure has been described in detail elsewhere [22]. In summary, distilled furfuryl alcohol was mixed with oxalic acid (100:3, w/w) at room temperature. Carbon synthesis required a continuous argon gas flow during mixture polymerisation (150 °C; 1h) and subsequent carbonization (800 °C; 2h). The resulting char was removed from the furnace then ground and sieved (≈ 100 µm). These particles were then subjected to a repeated, cyclic oxygen-argon activation procedure: oxygen atmosphere chemisorption (250 °C; 8h); desorption under argon atmosphere (800 °C; 2h); 9 cycles = 45% burn-off. The structural evolution of the adsorbent along the activation pathway has been examined in detail [21], along with the chemistry and surface properties of the sample [7].

Liquid adsorptives used in this study, their grade, and supplier details are given in Table 1. These same molecules are plotted with their kinetic diameter as a function of their dipole moment in Fig. 1. For comparison, a set of frequently used non-polar adsorptives are also included [2].

Table 1 Adsorptives, their physical properties, and conditions used for adsorption experiments

Adsorptive	Molecular Weight (kg/kmole)	Liquid Density at ads Temp. (g/cm^3) [24, 25]	Minimum Kinetic Diameter (nm) [20, 26]	Dipole Moment (D) [27]	Grade / Supplier[#]
Water (H_2O)	18.0	1.000	0.27	1.8	Milli-Q water
Dichloromethane (DCM)	84.9	1.33	0.33	1.8[†]	CHROMASOLV Plus > 99.9 % / SA
Pyridine	79.1	0.982	0.37	2.2	HPLC Grade > 99.9 % / SA
Methanol (MeOH)	32.04	0.792	0.43	1.7	Analysis grade > 99.9 % / M
Iso-propanol (iso-PrOH)	60.1	0.785	0.47	1.7	HPLC Grade > 99.9 % / SA
2-methyl, 2-butanol (2M2B)	88.15	0.815	0.60 *	1.9	Analytical standard > 99.5 %, SA

* Kinetic diameter for this adsorptive was assumed equivalent to that of *t*-butanol

[†] The authors recognize this dipole moment is sometimes cited as 1.14 D and as 1.4 D

[#] SA = Sigma-Aldrich, USA; M = Merck, USA

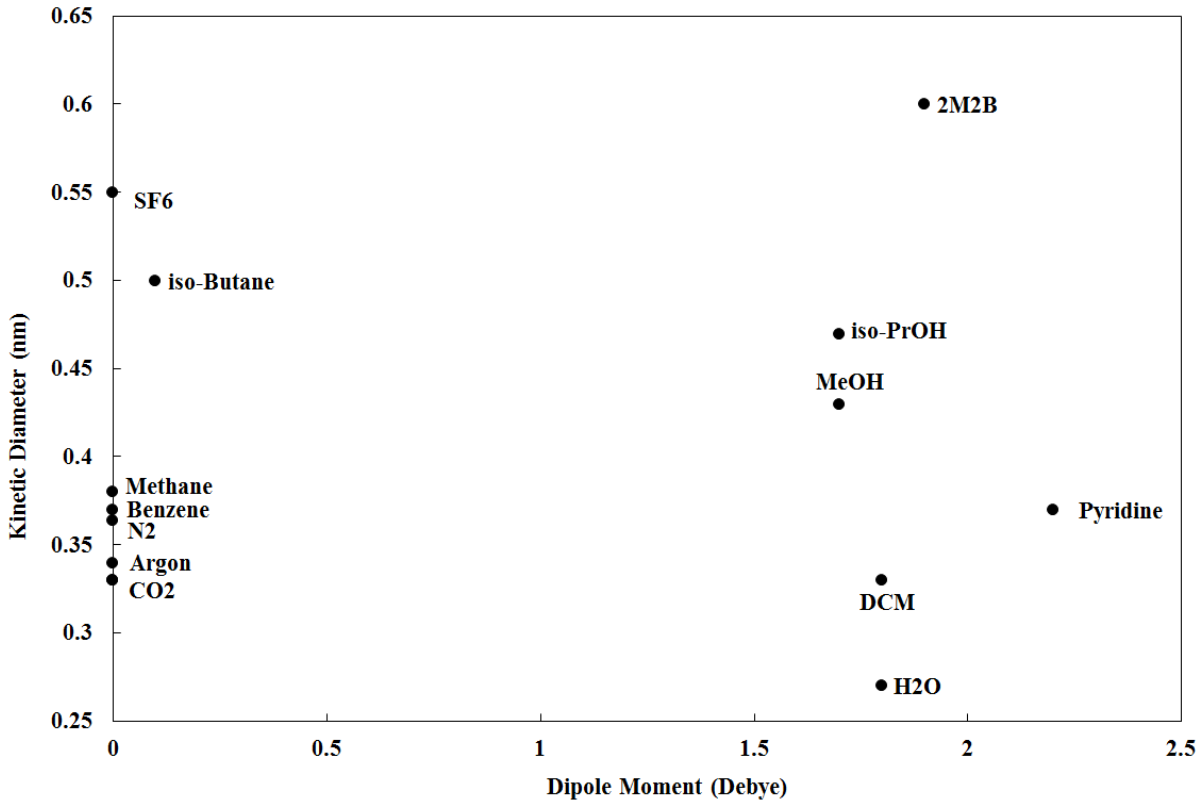

Fig. 1 Polar adsorptives used for adsorption experiments, their kinetic diameters and dipole moments; non-polar adsorptives included for comparison [2]

Each sample was degassed (250 ^{o}C; 4 h; 10^{-5} kPa) prior to adsorption isotherm measurements. Helium was used for dead-space corrections (> 99.999%, ex. BOC Gases, Adelaide, Australia). All adsorption isotherms were obtained using a BELSORP-max gas adsorption apparatus (BEL, Osaka, Japan) equipped with a vapor adsorption kit and combined with a Neslab refrigerated bath circulator with temperature control as 298.00 ± 0.01 K. For each adsorptive, isotherms were measured on three separate samples, and an average and standard deviation was used for discussions and analyses. As previously, one of the three isotherms for each adsorptive was chosen arbitrarily as the primary and the remainder were normalised to it. Separate normalisation of each measured equilibrium relative pressure and associated amount adsorbed was achieved using a MATLAB cubic Hermite interpolation polynomial subroutine. The weighted average values and their combined standard uncertainties were developed by propagating the uncertainty in each separate value [28].

RESULTS and DISCUSSION

Previous adsorption analyses of this carbon focused on non-polar adsorptives whose predominant mode of interaction would be non-specific, but with fluid-fluid interactions sufficient to promote condensation within the micropores [2]. It would be clear from the details in Fig. 1 that the adsorptives used in this work offered a kinetic diameter range consistent with their non-polar counterparts, *viz*. 0.27-0.60 nm compared with 0.33-0.55 nm. Additionally, Gurvitsch-type pore volumes for specific molecules could be compared directly with their non-polar counterpart to rationalise the influence of adsorbent surface chemistry and adsorptive polarity on the initial and possibly overall adsorption mechanism, resulting isotherm shape, and total volume adsorbed. This approach complements the works presented in the Introduction [17, 18]. From an adsorptive kinetic diameter perspective, a direct comparison of pyridine adsorption with benzene adsorption would be most beneficial, however it should also be noted that pyridine has been classified as a Lewis base [29], possibly promoting chemisorption with surface functional groups [30].

i. Pore volume analyses

The adsorption isotherm for each adsorptive listed in Table 1 is shown in Fig. 2 with the amounts adsorbed converted to liquid-like volume adsorbed. As the basis adsorptive for comparison and analysis in this work, the nitrogen adsorption isotherm was also included. The combined standard uncertainty in each amount adsorbed, developed from the triplicate isotherm analyses, was included at medium and high pressures, and those near saturation pressures were within the ranges reported elsewhere for specific pore volume calculations [31, 32]. The combined standard uncertainty in relative pressure data were excluded at high pressures for clarity. The N_2 isotherm exhibited the Type I shape based on the IUPAC classification [33], validating previously published results for this carbon

[22], and confirming the sample in this work also had primarily microporous structure with negligible contributions to the total amount adsorbed from mesoporosity and/or from any external surface [33]. The PSD calculated from a QSDFT application confirmed this supposition, indicating a narrow, primary distribution of pores centred at 0.57 ± 0.05 nm, also consistent with previous studies based on repeated isotherm measurements [22] and on model-independent methods such as calorimetry and isosteric heat analyses [20, 34, 35].

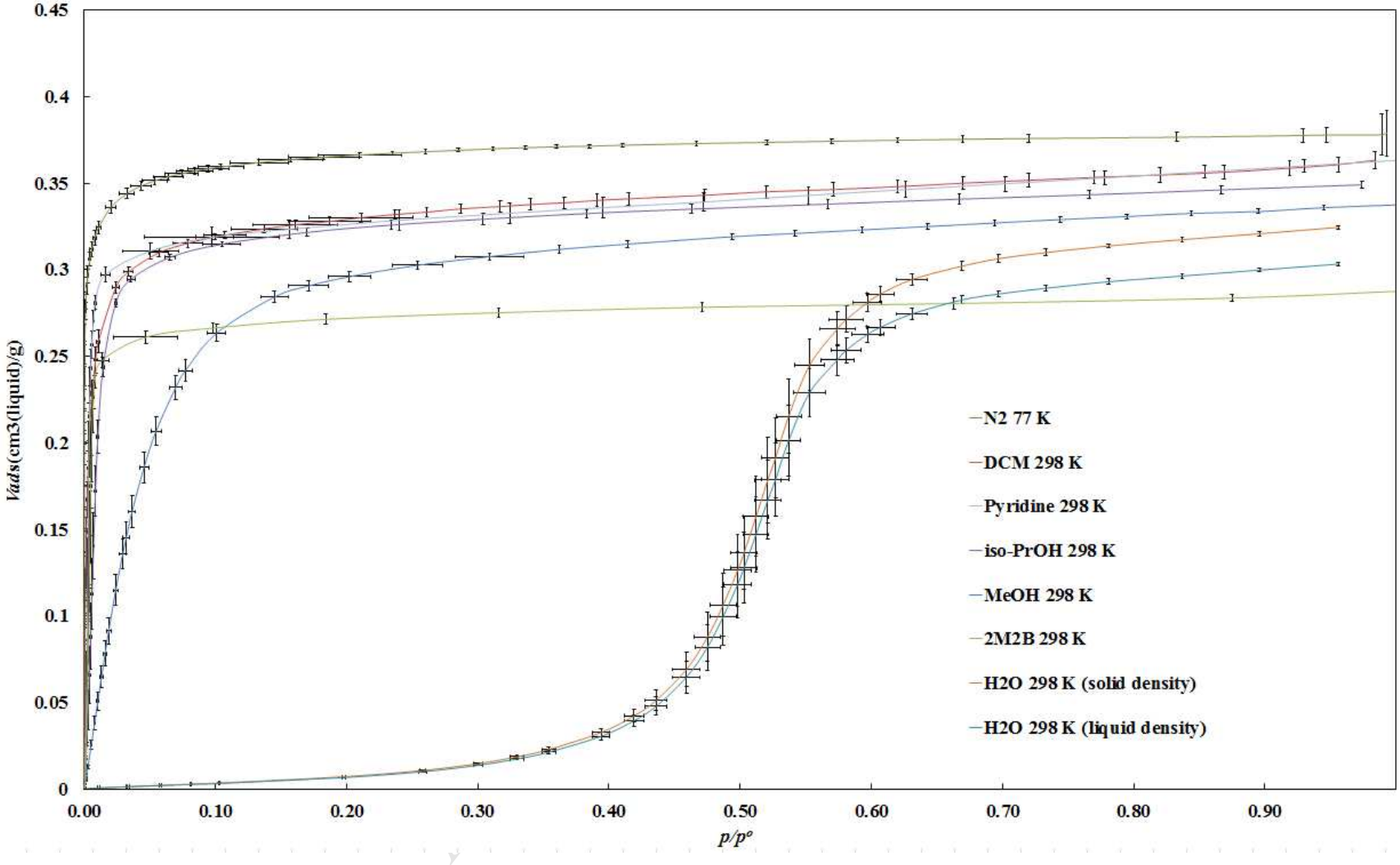

Fig. 2 Adsorption isotherms for the polar adsorptives listed in Table 1 and for nitrogen on PFA-based microporous carbon samples. Isotherm temperatures for each as listed in the inset legend. The two isotherms for water demonstrate the adsorbate (equivalent) density effect on volume adsorbed (online colour version is available).

Isotherms classified as Type I, IV, and V [33] often exhibit a plateau parallel to the p/p^o axis, especially at pressures approaching saturation for the isotherm temperature. It is generally assumed that at these pressures all micropores (and mesopores if present) would be filled with liquid-like adsorbate, and the liquid volume adsorbed would be equivalent to the available pore volume, v_p, the Gurvitsch volume. Differences in the amounts adsorbed in the current work as $p/p^o \rightarrow 1.0$ suggests that these micropore volumes would approximate adsorptive dimension-controlled, specific micropore volumes, molecular sieve exclusion effects defined as criterion 1 above.

Differences in evaluated Gurvitsch volumes are not necessarily attributable to adsorptive dimensions alone; molecular packing effects themselves manifest as an effect due either to dependence on the critical ratio of adsorptive size: pore size [20] or to long-range structure development in the adsorbed phase within pores of suitable dimensions. These influences are expressed by both non-polar [2] and polar molecules in the adsorbed phase, defined as criterion 2 exclusion effects. The concept of a critical ratio between adsorptive dimensions and pore dimensions affecting adsorbed phase packing derives from the proximity of the mean pore size to the adsorptive's kinetic diameter. These effects were proposed by Brunauer *et al* [36], supported by Rege and Yang [37], and more recently confirmed by immersion calorimetry studies of this PFA-based carbon (mean pore width = 0.57 ± 0.05 nm) into MeOH and *iso*-PrOH [20]. These enthalpy measurements suggested there was a negligible influence of packing effect during adsorption filling for MeOH since its kinetic diameter (0.43 nm) was considerably smaller than the mean pore size. In contrast, the combination of different molecular conformation and subtle increase in kinetic diameter for iso-PrOH (0.47 nm) resulted in reduced immersion enthalpy. Overall, the calorimetry measurements discerned molecular packing influences would be critical when the adsorbate kinetic diameter ranged between 0.5 – 1 times mean pore size. This observation differed considerably from Gurvitsch volume conclusions that adsorbate packing influences were critical when the ratio of pore width-to-adsorbate diameter ≤ 4 [38].

Hydrogen bonding and Lewis acid-base interactions within the adsorbed phase would be exemplars of mechanisms for long-range structure development. Consider water as the adsorptive, with a kinetic diameter of 0.27 nm, significantly smaller than those for MeOH (0.43 nm) and 2M2B (0.60 nm), but the amount adsorbed was intermediate these two adsorptives, regardless of whether the adsorbed phase were taken as liquid-like or solid-like [39-41]. The water dipole moment at 1.8 D was also intermediate those for MeOH (1.7 D) and 2M2B (1.9 D). Clearly, each adsorptive appears to have an approximately equivalent capacity to form intermolecular hydrogen bonding (as 1.8 ± 0.1 D ≈ ± 5.6%), stimulating 3-dimensional structure within the adsorbed phase. The small-valued relative difference (5.6%) in the average dipole moment for these three adsorptives (1.8 0.1 D) suggests each would have an equivalent capacity to form 3-dimensional hydrogen bonded structure when filling pores of appropriately large dimensions. For those micropores with dimensions sized similar to

the adsorptive, these intermolecular interactions within the adsorbed phase would lead to 2-dimensional adsorbate structure formation. This structure formation produces a lower space-filling efficiency than 3-dimensional structure filling resulting in greater occluded volume ("unfilled" pore space). The carbon adsorbent herein, and most activated carbon adsorbents contain a distribution of micropore width and thus, pore volume filling efficiency would be reduced by combinations of size exclusion and adsorbed phase structure formation. These effects combine to provide reduced Gurvitsch volume adsorbed. This phenomenon is defined as criterion 3 above.

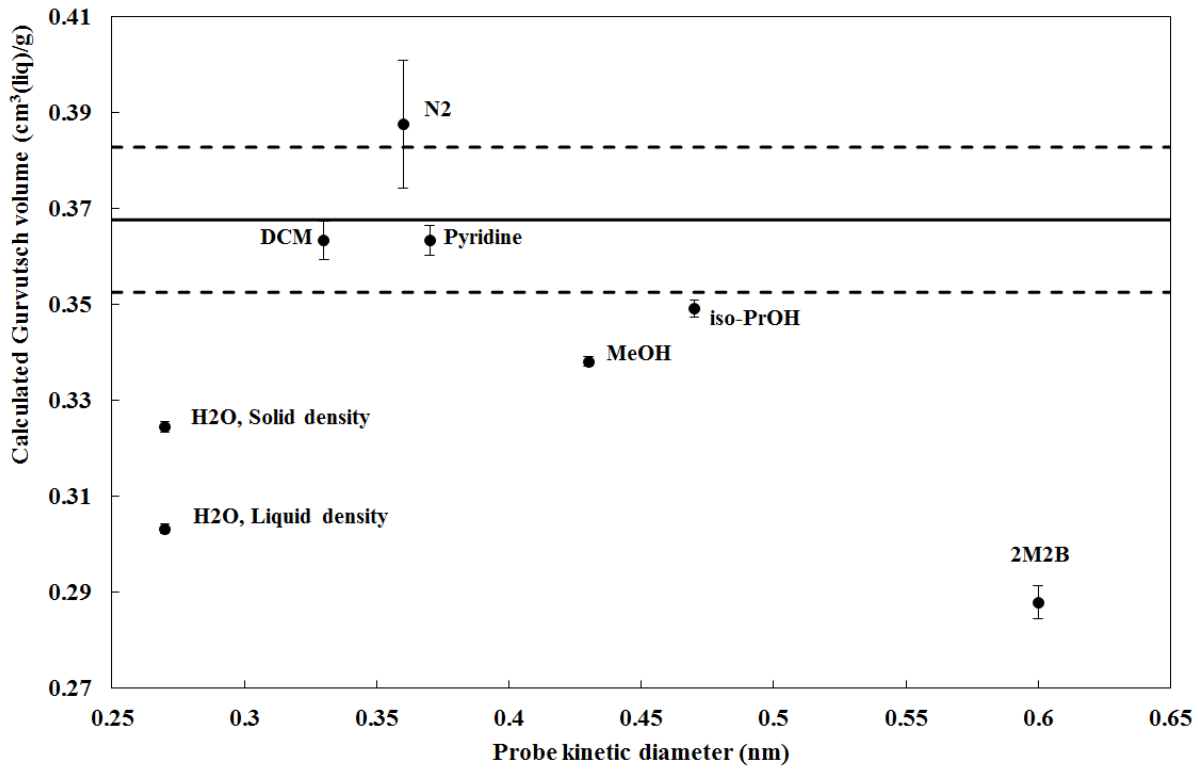

Fig. 3 Calculated Gurvitsch volume for selected probes as a function of their kinetic diameter. Average Gurvitsch volume of non-polar adsorptives (N_2, Ar, CH_4, and C_6H_6) [2] (—); standard deviation of the average Gurvitsch volume (---)

The proposed average Gurvitsch volume for this PFA-based carbon was evaluated using the non-polar adsorptives N_2, Ar, CH_4, and C_6H_6 as 0.368 ± 0.015 cm^3(liq)/g with an average micropore width of 0.57 ± 0.05 nm. The kinetic diameter of each polar adsorptive in Table 1 suggests that each would penetrate some, if not all of the pores; the Gurvitsch volumes for these were imprinted over the average volume in Fig. 3. Interestingly, only DCM and pyridine produced pore filling to an extent statistically coincident with the accepted Gurvitsch volume, and thus exhibited independence of the criterion classified as molecular sieve exclusion effects, criterion 1. Previous immersion calorimetry analyses showed no molecular packing effects for probes with similar dimensions, including DCM [20], implying that these adsorptives were also independent of the criterion defined above as

molecular packing exclusion effects, criterion 2. Although both have strong dipole moments, 1.8 and 2.2 D respectively, neither is susceptible to hydrogen bonding. Of course, pyridine is a Lewis base [29] but, since the Gurvitsch volume was statistically equivalent to the accepted volume, the pores probably contained no Lewis acid sites that might have promoted 2- or 3-dimensional structure within the pores. The presence of the chlorine atoms in DCM reduces the kinetic diameter (0.33 nm) compared with its fully hydrogenated counterpart, methane with diameter 0.38 nm. Both molecules provided statistically equivalent Gurvitsch volumes, 0.371 cm^3(liq)/g for CH4 and 0.365 cm^3(liq)/g for DCM. Thus, these adsorptives were independent of the criterion defined above related to 2- and/or 3-dimensional structure formation in the adsorbed phase leading to occluded volume within the filled pores, as exclusion effect criterion 3.

Water with a kinetic diameter of 0.26 nm and MeOH at 0.43 nm would be expected to exhibit independence of molecular sieve effects (criterion 1), penetrate all pores and produce Gurvitsch volumes akin to the accepted value. Immersion calorimetry measurements supported the argument that packing exclusion effects (criterion 2) would also not be a factor [20]. Clearly, from Fig. 3 neither expectation was met. Since both adsorptives have similar dipole moments and hydrogen bonding capability, an interpretation would be that their adsorbed phases contained significant occluded volume due to 2- and/or 3-dimensional structure formation, i.e. their adsorption was subject to the structure-formation exclusion effect, criterion 3. The molar volume of ice > water at 298 K; applying the former increased the Gurvitsch volume suggesting a marginal decrease in occluded volume if an ice-like phase were to better describe the adsorbed phase within the micropores of this PFA-carbon. No immediate investigations were made to expand our interpretation of this difference. The Gurvitsch volume for MeOH at 0.338 cm^3(liq)/g showed less deviation from the accepted average Gurvitsch volume as 0.368 ± 0.015 cm^3(liq)/g, suggesting hydrogen bond-influenced, long-range structure formation within the adsorbed phase was possibly weaker compared to water, and thus the near equivalence of the volumes. Secondly, the melting point of MeOH is ≈ 175 K, a temperature (probably) too low to invoke a solid-like adsorbed phase of MeOH for the adsorption 298 K. Clearly, further measurements and/or adsorption simulations would be necessary to clarify the differences between H_2O and MeOH adsorption. More than likely, van der Waals or dispersion force contributions from the methyl group would enhance the adsorption process beyond specific adsorption. Specific and dispersion force interactions, as simultaneous interactions would be an equivocal variable for such modelling." Again linguistic care towards a more clear explanation of the authors' ideas is required.

The kinetic diameters for *iso*-PrOH and 2M2B are close to the mean pore width of 0.57 nm, suggesting one would expect some molecular sieve exclusion effects to prevail. The Gurvitsch volume for *iso*-PrOH was marginally lower than the accepted pore volume whereas that for 2M2B

was significantly (approximately 15%) lower, suggesting molecular sieve exclusion effects prevailed and the reduction could be designated as criterion 1 volume losses. Recent immersion calorimetry measurements for the PFA-carbon into these solvents were interpreted as adsorptives of dimensions approaching the size designated as the critical pore-to-adsorptive ratio, leading to critical molecular packing effects in selected micropores and to exclusion as per criterion 2 volume losses. Additionally, both adsorptives possess sufficient polarity to promote hydrogen bonding within the adsorbed phase. As per the arguments presented above for MeOH, for these adsorptives, two simultaneous mechanisms of adsorption could occur: van der Waals or dispersion force interactions via the alkane moieties in the adsorptives; non-dispersion force interactions, as hydrogen bonding, via the alcohol functional group in the adsorptives. The latter interaction could lead to occluded volume within the adsorbed phase, contributing to criterion 3 volume exclusion losses.

An alternative and reasonably well-accepted method for micropore volume evaluation was that developed by Dubinin and Radushkevich [14]. The DR equation (1) defines pore volumes for classical Type I adsorption isotherms, but Dubinin stressed that the TVFM was most suitable to pore filling exceeding 0.1 V_{mic}, where V_{mic} = the total micropore volume. Nonetheless, the DR model finds widespread application for micropore filling analyses at low relative pressures:

$$\log\left(V_{ads}\right) = \log\left(V_{mic}\right) - D\log^2\left(p^o/p\right) \qquad (1)$$

The coefficient D is an empirical representation of the free energy of adsorption of the examined adsorptive, hence referred to in the TVFM as the characteristic free energy of adsorption. The influence of specific interactions as the primary adsorption interactions, typically encountered in pore fillings < 0.1 V_{mic}, results in adsorptive-dependent, non-linearity in a log (V_{ads}) – $\log^2(p^o/p)$ plot across an extended (low) relative pressure range, leading to the general acceptance that the DR model fails to adequately fit polar molecule adsorption isotherms [13]. Consequently, one would be correct to criticise its application to the adsorptives considered herein.

If the adsorbing micropores were sufficiently wide to accommodate an initial “monolayer-type” pore filling mechanism (*layering*), followed by condensation over a relatively narrow relative pressure range, then a plot of Eq. (1) would exhibit a linear range encompassing the condensation process, highlighting a unique micropore volume. Fig. 4 shows said plots including uncertainty in each datum; linear ranges were evident. For each adsorptive, micropore volumes were evaluated via a weighted linear least squares analysis giving uncertainty in slope and intercept, as presented in Table 2 beside Gurvitsch volumes. These results show a modest agreement between the two methods of evaluation. It was clear that the increasing polar nature of the adsorptives rendered greater deviation from linearity,

however in most cases suitable ranges were identified. No linear section was suitably identified for the highly specific adsorptives H_2O and MeOH, unique pore volume analyses failed.

Clearly, the classification of adsorptives as polar and non-polar is helpful, but not comprehensive, since the mechanism of interaction with the surface would depend on both adsorptive polarity and probability of specific and/or nonspecific interactions. For example, the physical properties of the water molecule, small size, high polarity, and highly electronegative oxygen atom proffer specific interactions and negligible affinity for nonspecific interactions. Fig. 4 shows that the DR plot for this probe was non-linear. Conversely, methanol offers the polarisable alcohol group for specific interactions with the same polar surface sites and the methyl group for nonspecific interactions with the predominantly carbon surface atoms. Furthering this comparison, as the number of carbons in the alkyl group increases to 3 and 4 (*iso*-PrOH and 2M2B), the nonspecific interaction potential increases and the DR plots for these would exhibit wider ranging linearity. Subsequent analysis of these results (below) will show that although polar probe DR plots are generally non-linear, its application can significantly enhance our understanding of the pore filling and specific vs. nonspecific interaction contributions to the pore filling process.

Table 2 Calculated pore volumes via DR method and comparison with Gurvitsch volume

Adsorptive	Gurvitsch volume ($cm^3. g^{-1}$)	DR volume ($cm^3. g^{-1}$)*
N_2	0.388±0.013	0.373
DCM	0.363±0.004	0.347
Pyridine	0.363±0.003	0.347
iso-PrOH	0.349±0.002	0.361
MeOH	0.338±0.001	-
2M2B	0.288±0.003	0.276
H_2O	0.324±0.001	-

* The evaluated relative uncertainties for the data were exceptionally small. The average relative uncertainty was (2.63±4.06) x 10^{-4} cm^3/g

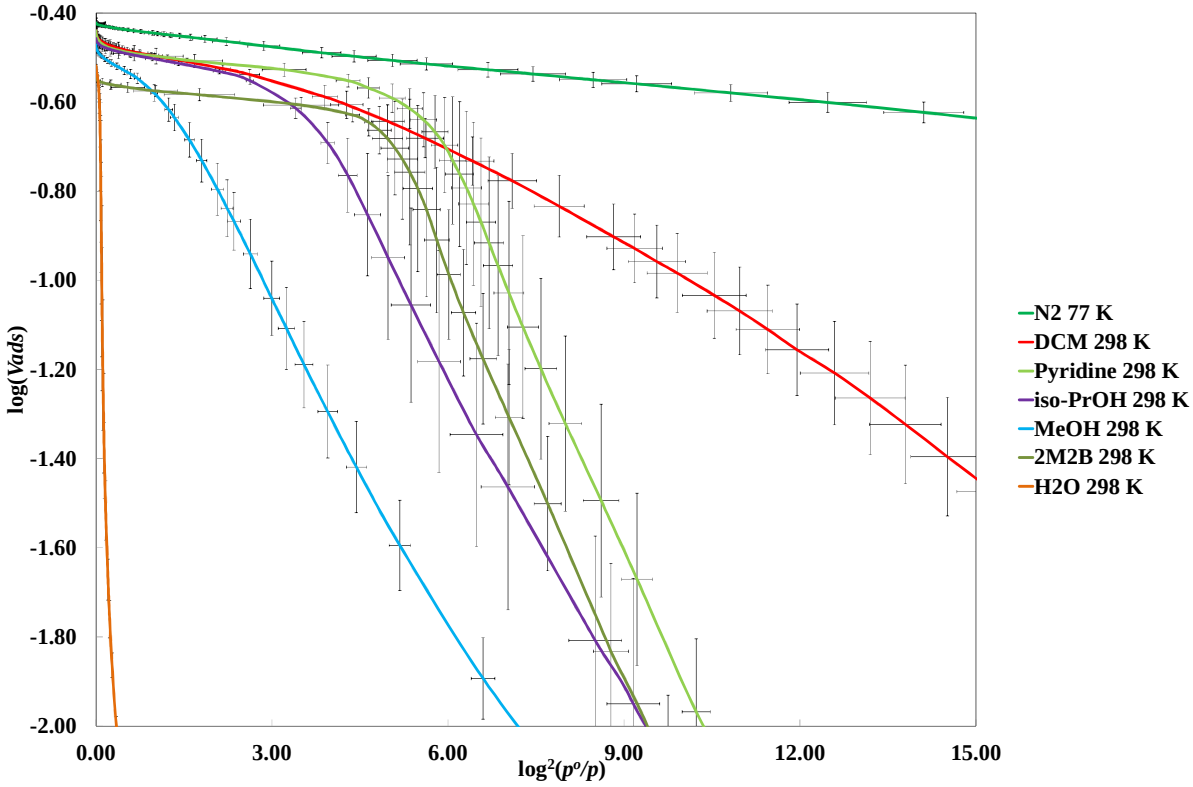

Fig. 4 DR plots for the adsorptives listed in Table 1 (online colour version is available).

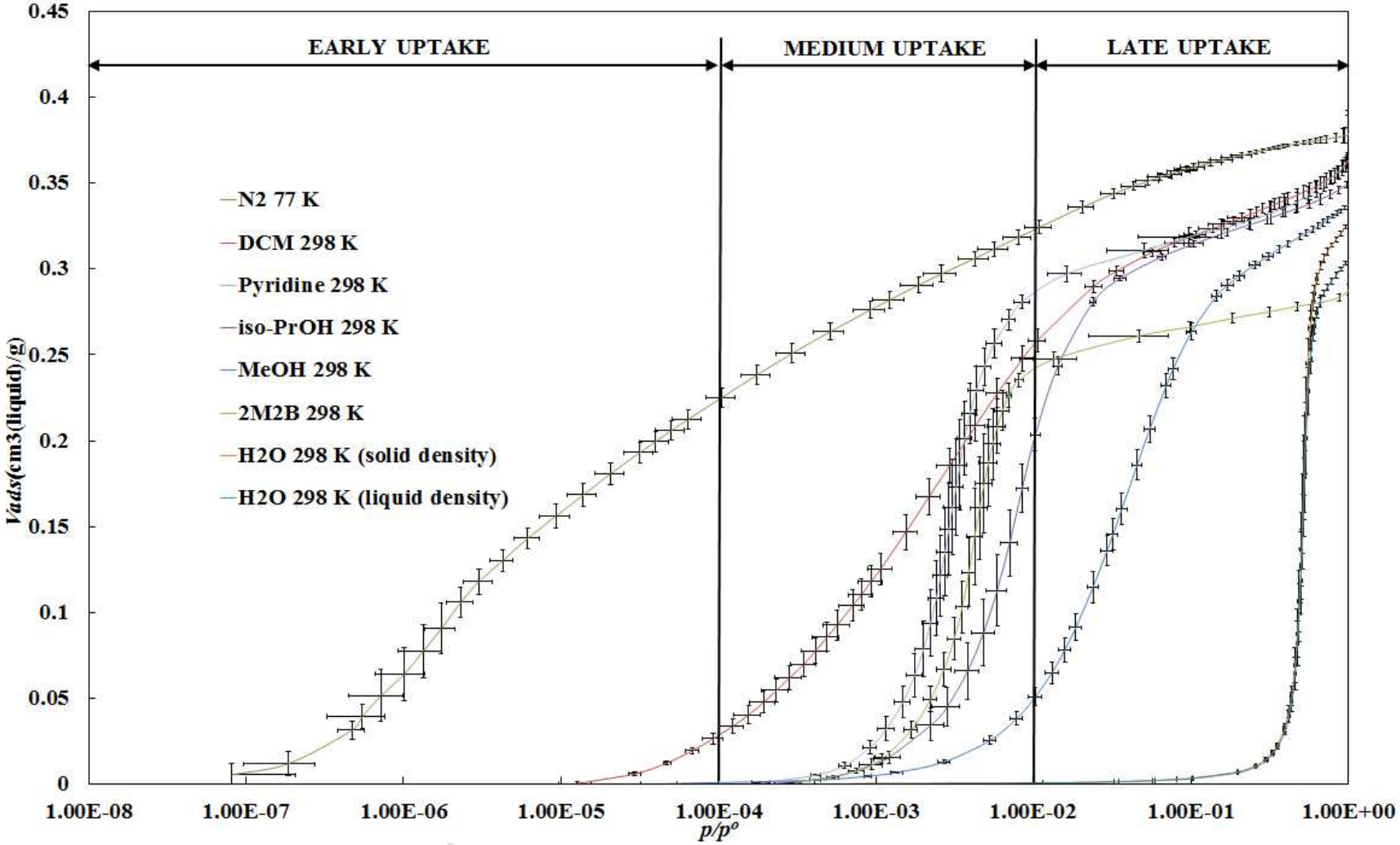

Fig. 5 Log-scale adsorption isotherms for the polar adsorptives listed in Table 1 on PFA-based microporous carbon samples. Nitrogen isotherm included as basis. Uptake relative pressure ranges: early uptake: 1×10^{-8} - 1×10^{-4}; medium uptake: 1×10^{-4} - 1×10^{-2}; late uptake: 1×10^{-2} – 10^{0}(=1) (online colour version is available)

ii. Isotherm shape analyses

Fig. 5 presents the averaged adsorption isotherms for the polar adsorptives in Table 1 on a log-scale p/p^o axis, clarifying the influence of possible polar or polarisable surface groups on the initial amount adsorbed. Apart from the water adsorption isotherms, each of the adsorptives exhibited the classical Type I character for the linear-scale p/p^o axis, supporting the duplication of plotting the isotherms for qualitative analysis purposes. The inclusion of the propagated, combined standard uncertainty in the averaged relative pressures and their dependent amounts adsorbed highlight qualitatively the regions of sensitivity within adsorption isotherm results. The combined standard uncertainties in the relative pressures are largest in the low pressure ranges of the isotherm, primarily an indication of the sensitivity of the pressure gauges in the equipment. The combined standard uncertainty in those isotherms showing rapid uptake over a relatively short relative pressure range also show the sensitivity of the measurements [42]. As presented previously, a qualitative comparison of the isotherms in the logarithmic format highlights the relative differences in the adsorption mechanism and associated thermodynamics for pore filling by each adsorptive.

Although each isotherm was measured on the same equipment with the same pressure sensors, each isotherm shows considerably different lowest relative pressure detection limits for reliably measureable amounts adsorbed. Each of the polar adsorptives show S-shaped character and clearly definable ranges over which condensation had occurred within the micropores, with some over narrower relative pressure ranges than others. At relative pressures above the "critical micropore filling" conditions, the isotherms exhibit reasonably similar shape, interpreted as adsorption by those pores on the extremity of the PSD becoming equivalent to external surface. The fineness of the relative pressure range for condensation within the micropores is an indication of either the intermolecular packing or the intermolecular interactions defined broadly as "polarity-induced bonding" within the adsorbed phase, or their combination. In contrast, the wide relative pressure range over which micropore filling occurred for nitrogen was an example of relatively weak fluid-fluid or intermolecular interactions within the adsorbed phase. In Fig. 4 the polar adsorptives showed deviation from linearity in their DR plots whereas nitrogen showed extensive linearity. Overall, linearity was interpreted as an indication that pore filling was a *layering* and/or *condensation* phenomenon.

As shown previously for non-polar adsorptives, it was possible to further classify and refine the isotherms in Fig. 5 by relative pressure-controlled micropore filling or uptake ranges: **early**, $p/p^o = 10^{-8}$ - 10^{-4}; **medium**, $p/p^o = 10^{-4}$ - 10^{-2}; and **late**, $p/p^o = 10^{-2}$ - 10^{0} (=1). These ranges specify adsorption processes suggested to be due to specific or non-specific interaction forces, due to adsorptive polarity and/or polarizability, and/or due to adsorptive molecular shape influences on the adsorption process in the micropores. The isotherms were further classified via these.

a) **Polar adsorptives with primarily specific interaction:** This class of adsorptives exhibit strong fluid-fluid interactions via hydrogen bonds, and relatively weaker fluid-solid interactions. Examples include 2M2B, *iso*-PrOH, MeOH, and H_2O. Of the organic molecules in this list, adsorption could occur specifically via the alcohol functional group or more generally via the alkyl moiety. Specific interactions would occur with other polar or polarisable surface functional groups and, depending on the relative strength of such interactions, further polarisation within the molecule could lead to localised adsorption via induced polarity or via hydrogen bonding within the adsorbed phase followed by adsorbate cluster formation. Weaker dispersion force interactions would occur on other locations of an adsorbent surface [43].

Each of the above examples contains a large dipole moment: 1.9 D for 2M2B, 1.7 D for both *iso*-PrOH and MeOH, and 1.8 D for water. Adsorption of either of these molecules would be initially on the pore surface containing functional groups defined as high energy sites (HES), assuming steric effects were absent [35]. Subsequent adsorptive molecules would interact with the adsorbate via hydrogen bonding creating localised adsorbed-phase clusters. A limited number of such sites on any given surface would result in low amounts adsorbed at the lowest measured pressures, increase in size with increasing pressure, eventually leading to inter-cluster coalescence, pore filling as condensation, and a relatively sharp increase in the amount adsorbed over a relatively narrow pressure range. From Fig. 5, it is clear that the equilibrium pressure at which such condensation occurs was adsorptive polarity and specific interaction force dependent, consistent with previous observations [18].

The dipole moment of the adsorptive was not the only indicator of adsorption. The prevalence for specific interactions diminished with increasing size of alkyl group in the adsorptive molecule, which, for the above adsorptives the classification was: water > MeOH > *iso*-PrOH > 2M2B, matching the order of increasing relative pressure for adsorption condensation to occur in Fig. 5. The condensation processes occurred at adsorptive phase relative pressures > 10^{-3}, the higher-valued medium and late uptake categories. Similar trends were evident in the DR plots. Water, with its negligible possibility for non-specific interactions with carbon surfaces showed the largest deviation from linearity. MeOH shows a capacity for specific and non-specific interactions; its large departure from linearity in DR plots confirmed specific adsorption interactions over non-specific interactions. In the case of *iso*-PrOH and 2M2B, their relatively larger alkyl groups raised the probability for non-specific interactions resulting in more clearly defined linear ranges across a relatively broad range of pressures.

b) **Polar adsorptives with potential for non-specific interaction.** This class of adsorptives would be similar to those above, but the prospects for non-specific or dispersion force dependence increase with increasing carbon content, if the adsorptive were organic-based. Examples include

iso-PrOH, 2M2B, and pyridine. As above, for alcohols, the alcohol functional group would experience specific interactions with HES, while the alkyl moiety would promote dispersion force interactions with an adsorbent surface and within the adsorbed phase as relatively weak fluid-fluid interactions, increasing in importance as the alkyl chain length increases.

Pyridine also exhibits a large dipole moment, 2.2 D, due to the lone pair of electrons on the nitrogen atom in this flat, relatively inflexible molecule. The aromatic π-electron character of this adsorptive promotes dispersion force interactions with adsorbents while the lone pair of electrons has this molecule classified as a Lewis base [29], promoting specific interactions. Molecules such as this exhibit shape and uptake in the medium pressure range, due to (almost simultaneous) *clustering* and *layering* adsorption mechanisms, with structure formation within the adsorbed phase. *Clustering* would be deduced as deviation from linearity at low pressures (high $\log^2(p^o/p)$) in a DR plot whereas *layering* would be equated with linearity at high pressures. Overall, the nature of the interaction would be somewhat governed by the number and type of functional groups decorating the adsorbent surface. For this PFA-based carbon, the number density of HES was low and thus the position of the condensation relative pressure range was similar to that for 2M2B, suggesting that the nitrogen moiety of the former and the alcohol group on the latter were susceptible to similar strength of non-dispersion forces for adsorption.

c) **Halogenated adsorptives:** Halogenated adsorptives offer interesting characteristics as surface and porosity probes. Chlorinated hydrocarbons are infrequently used as probes for adsorption mechanism analysis, but have been used to define PSD [44]. The electronegative nature of the halogen atoms induces dipolar properties within the molecule and thus a propensity for specific adsorption with HES or moderately polarisable surface groups, depending on the halogen atom and to what it were originally bonded. Adsorption of molecules with configurations similar to DCM would be expected to consist of both specific interactions via the halogen atoms and non-specific interactions via the alkyl group; one would predict a delayed, sharp uptake akin to water.

Although halogenated molecules have the potential to promote polarisation of surface sites, in the case of DCM in Fig. 5, the uptake with relative pressure change showed broad-range pressure dependence similar to the dispersion force, non-specific adsorption mechanisms presented previously. Adsorption began at low relative pressures, in the early uptake regime, similar to non-polar probes, implying possible non-specific interactions between the carbon-rich surface and the methylene component of the molecule. Adsorption and pore filling extended across the medium uptake regime and continued into the late uptake regime. Previous molecular dynamics analyses indicate that DCM exhibits an adsorbed phase structure in the liquid state, supporting the conclusion of fluid-fluid interactions across this pressure range [45]. Clearly, DCM behaved

intermediate polar and non-polar adsorptives where the DR analysis exhibited neither a marked (expectedly extended) deviation from linearity nor an extensive linear range of pressure.

CONCLUSIONS

Repeated adsorption isotherms of a set of selected polar adsorptives were reported and (1) quantitatively analysed and compared for pore volume measurements using both Gurvitsch volume and DR methods, and (2) qualitatively discussed isotherm shapes to deduce pore filling and adsorption mechanisms. The main conclusions are:

- Triplicate-measured, high resolution isotherms showed repeatable results with relatively small standard deviations in amounts adsorbed at low relative pressures.
- Adsorptives with kinetic diameter exceeding available pore widths exhibited molecular sieve effect contributions to diminished Gurvitsch volumes. For adsorptives of critical kinetic diameters, a reduced Gurvitsch volume was related to molecular packing effect in micropores. For adsorptives with the hydrogen-bonding potential, the reduced Gurvitsch volume was affected by 2D hydrogen bonding inside micropores. The observations were substantiated by DR analyses.
- The mechanism of adsorption and pore filling depended on the extent of fluid-fluid and fluid solid interactions. The adsorption isotherm shape, when plotted on a log relative pressure axis, could be classified into three groups:
    a- Polar adsorptives with primarily specific interactions (*iso*-PrOH, MeOH, 2M2B, H_2O); the adsorption mechanism follows cluster formation around available high energy sites on the solid surface at low pressures followed by condensation in the late uptake range. Specific interactions were highlighted by location and extent of non-linear response in DR analyses.
    b- Polar adsorptives with the potential for non-specific interactions (pyridine, *iso*-PrOH, 2M2B); the adsorption mechanism follows a combination of cluster formation on high energy sites and simultaneous adsorption via fluid-solid interactions and layering effects at low pressure, followed by condensation in the late uptake pressure range. *Clustering* would be deduced as deviation from linearity at low pressures (high $\log^2(p^o/p)$) in a DR plot whereas *layering* would be equated with linearity at high pressures..
    c- Halogenated adsorptives (DCM); these polar adsorptives offer both specific interactions via electronegative halogen atoms and non-specific interactions via hydrocarbon groups. This combination of specific and non-specific interactions was substantiated by DR analysis, illustrated by neither a marked deviation from linearity

nor an extensive linear range of pressure. Adsorption isotherms of these molecules would show an early uptake (like non-polar adsorptives) and a late uptake (like polar adsorptives), but overall, the isotherm would show a broad uptake over an extended pressure range.

ACKNOWLEDGEMENTS

The authors thank the Australian Research Council discovery program (DP110101293) for funding support and S.H.M also thanks the University of South Australia for a postgraduate research scholarship.

REFERENCES

[1] G. Mason, A model of adsorption-desorption hysteresis in which hysteresis is primarily developed by the interconnectivity in a network of pores, Proc. R. Soc. London, Ser. A, A390 (1983) 47.
[2] S.H. Madani, P. Kwong, F. Rodrígues-Reinoso, M.J. Biggs, P. Pendleton, Decoding gas-solid interaction effects on isotherm shape: I. non-polar adsorptives, In Press: Microporous and Mesoporous Materials, (2018).
[3] H. Marsh, F. Rodríguez-Reinoso, Activated Carbon, Elsevier Science2006.
[4] M.M. Dubinin, V.V. Serpinsky, Isotherm equation for water vapor adsorption by microporous carbonaceous adsorbents, Carbon, 19 (1981) 402-403.
[5] C. Pierce, R.N. Smith, The Adsorption–Desorption Hysteresis in Relation to Capillarity of Adsorbents, J. Phys. Colloid Chem., 54 (1950) 784-794.
[6] L. Liu, S. Tan, T. Horikawa, D.D. Do, D. Nicholson, J. Liu, Water adsorption on carbon - A review, Advances in Colloid and Interface Science, 250 (2017) 64-78.
[7] S. Sedghi, S.H. Madani, C. Hu, A. Silvestre-Albero, W. Skinner, P. Kwong, P. Pendleton, R.J. Smernik, F. Rodríguez-Reinoso, M.J. Biggs, Control of the spatial homogeneity of pore surface chemistry in particulate activated carbon, Carbon, 95 (2015) 144-149.
[8] Y. Kaneko, K. Ohbu, N. Uekawa, K. Fujie, K. Kaneko, Evaluation of Low Concentrated Hydrophilic Sites on Microporous Carbon Surfaces with an X-ray Photoelectron Spectroscopy Ratio Method, Langmuir, 11 (1995) 708-710.
[9] T.J. Bandosz, J. Jagiełło, J.A. Schwarz, A. Krzyzanowski, Effect of Surface Chemistry on Sorption of Water and Methanol on Activated Carbons, Langmuir, 12 (1996) 6480-6486.
[10] V.M. Gun'ko, T.J. Bandosz, Heterogeneity of adsorption energy of water, methanol and diethyl ether on activated carbons: effect of porosity and surface chemistry, PCCP, 5 (2003) 2096-2103.
[11] I.I. Salame, T.J. Bandosz, Adsorption of Water and Methanol on Micro- and Mesoporous Wood-Based Activated Carbons, Langmuir, 16 (2000) 5435-5440.
[12] M.V. López-Ramón, F. Stoeckli, C. Moreno-Castilla, F. Carrasco-Marín, Specific and Nonspecific Interactions between Methanol and Ethanol and Active Carbons, Langmuir, 16 (2000) 5967-5972.
[13] M.M. Dubinin, Physical adsorption of gases and vapors in micropores, in: D.A. Cadenhead (Ed.) Prog. Surf. and Membr. Sci., Academic Press, New York, 1975, pp. 1-70.
[14] M.M. Dubinin, L.V. Radushkevich, On the equation of the characteristic curve for active coals, Doklady Akademii Nauk SSSR [Reports of the Academy of Sciences of the USSR], 4 (1947) 331-334.
[15] M.M. Dubinin, E.F. Polstyanov, Adsorption properties of carbon adsorbents. VII. Theoretical analysis of the experimental data on equilibrium adsorption of vapors of substances on activated charcoals with different microporous structures, Izv. Akad. Nauk, Ser. Khim., (1966) 793-801.
[16] A. Andreu, H.F. Stoeckli, R.H. Bradley, Specific and non-specific interactions on non-porous carbon black surfaces, Carbon, 45 (2007) 1854-1864.

[17] R.H. Bradley, B. Rand, On the Physical Adsorption of Vapors by Microporous Carbons, J. Colloid Interface Sci., 169 (1995) 168-176.
[18] F. Rodriguez-Reinoso, M. Molina-Sabio, M.A. Munecas, Effect of microporosity and oxygen surface groups of activated carbon in the adsorption of molecules of different polarity, The Journal of Physical Chemistry, 96 (1992) 2707-2713.
[19] F. Rodríguez-Reinoso, M. Molina-Sabio, M.T. González, Effect of Oxygen Surface Groups on the Immersion Enthalpy of Activated Carbons in Liquids of Different Polarity, Langmuir, 13 (1997) 2354-2358.
[20] S.H. Madani, A. Silvestre-Albero, M.J. Biggs, F. Rodríguez-Reinoso, P. Pendleton, Immersion Calorimetry: Molecular Packing Effects in Micropores, ChemPhysChem, 16 (2015) 3984-3991.
[21] C. Hu, A.C.Y. Liu, M. Weyland, S.H. Madani, P. Pendleton, F. Rodríguez-Reinoso, K. Kaneko, M.J. Biggs, A multi-method study of the transformation of the carbonaceous skeleton of a polymer-based nanoporous carbon along the activation pathway, Carbon, 85 (2015) 119-134.
[22] C. Hu, S. Sedghi, S.H. Madani, A. Silvestre-Albero, H. Sakamoto, P. Kwong, P. Pendleton, R.J. Smernik, F. Rodríguez-Reinoso, K. Kaneko, M.J. Biggs, Control of the pore size distribution and its spatial homogeneity in particulate activated carbon, Carbon, 78 (2014) 113-120.
[23] C. Hu, S. Sedghi, A. Silvestre-Albero, G.G. Andersson, A. Sharma, P. Pendleton, F. Rodríguez-Reinoso, K. Kaneko, M.J. Biggs, Raman spectroscopy study of the transformation of the carbonaceous skeleton of a polymer-based nanoporous carbon along the thermal annealing pathway, Carbon, 85 (2015) 147-158.
[24] C.F. Spencer, R.P. Danner, Improved equation for prediction of saturated liquid density, J. Chem. Eng. Data, 17 (1972) 236-241.
[25] R.H. Perry, D.W. Green, Perry's chemical engineer's handbook, McGraw-Hill, New York, 1999.
[26] Y. Yan, T. Bein, Molecular recognition on acoustic wave devices: sorption in chemically anchored zeolite monolayers, J. Phys. Chem., 96 (1992) 9387-9393.
[27] Bruce E. Poling, J. M. Prausnitz, J.P. O'Connell, The properties of gases and liquids, 5 ed., McGRAW-HILL, New York, 2001.
[28] J.R. Taylor, An Introduction to Error Analysis: The Study of Uncertainties in Physical Measurements, University Science Books, New York, 1982.
[29] R.S. Drago, G.C. Vogel, T.E. Needham, Four-parameter equation for predicting enthalpies of adduct formation, J. Am. Chem. Soc., 93 (1971) 6014-6026.
[30] F.M. Fowkes, Acid-base interactions in polymer adsorption, Ind. Eng. Chem. Prod. R&D, 17 (1978) 3.
[31] P. Pendleton, A. Badalyan, Gas adsorption data uncertainty and propagation analyses, Adsorption, 11 (2005) 61-66.
[32] A. Badalyan, P. Pendleton, Analysis of uncertainties in manometric gas-adsorption measurements: II. Uncertainty in -analyses and pore volumes, J. Colloid Interf. Sci., 326 (2008) 1-7.
[33] M. Thommes, K. Kaneko, V. Neimark Alexander, P. Olivier James, F. Rodríguez-Reinoso, J. Rouquerol, S.W. Sing Kenneth, Physisorption of gases, with special reference to the evaluation of surface area and pore size distribution (IUPAC Technical Report), Pure Appl. Chem., 87 (2015) 1051.
[34] S.H. Madani, C. Hu, A. Silvestre-Albero, M.J. Biggs, F. Rodríguez-Reinoso, P. Pendleton, Pore size distributions derived from adsorption isotherms, immersion calorimetry, and isosteric heats: A comparative study, Carbon, 96 (2016) 1106-1113.
[35] S.H. Madani, S. Sedghi, M.J. Biggs, P. Pendleton, Analysis of Adsorbate–Adsorbate and Adsorbate–Adsorbent Interactions to Decode Isosteric Heats of Gas Adsorption, ChemPhysChem, 16 (2015) 3797-3805.
[36] S. Brunauer, S. Mikhail, E.E. Bodor, Pore structure analysis without a pore shape model, J. Colloid Interface Sci., 24 (1967) 451.
[37] S.U. Rege, R.T. Yang, Corrected Horvath-Kawazoe equations for pore size distribution, AlChE J., 46 (2000) 734-750.

[38] F. Rouquerol, J. Rouquerol, K. Sing, Adsorption by powders and porous solids Academic Press, London, 1999.
[39] M. Thommes, C. Morlay, R. Ahmad, J.P. Joly, Assessing surface chemistry and pore structure of active carbons by a combination of physisorption (H2O, Ar, N2, CO2), XPS and TPD-MS, Adsorption, 17 (2011) 653.
[40] R.S. Vartapetyan, A.M. Voloshchuk, A.K. Buryak, C.D. Artamonova, R.L. Belford, P.J. Ceroke, D.V. Kholine, R.B. Clarkson, B.M. Odintsov, Water vapor adsorption on chars and active carbons–oxygen sensors prepared from a tropical tree wood, Carbon, 43 (2005) 2152-2159.
[41] T. Iiyama, M. Ruike, K. Kaneko, Structural mechanism of water adsorption in hydrophobic micropores from in situ small angle X-ray scattering, Chem. Phys. Lett., 331 (2000) 359-364.
[42] P. Pendleton, A. Badalyan, Gas adsorption data uncertainty and propagation analyses, Adsorption, 11 (2005) 61-66.
[43] J. Mahanty, B.W. Ninham, Dispersion forces, Academic Press, New York, 1976.
[44] R.K. Mariwala, H.C. Foley, Calculation of Micropore Sizes in Carbogenic Materials from the Methyl Chloride Adsorption Isotherm, Ind. Eng. Chem. Res., 33 (1994) 2314-2321.
[45] L.X. Dang, Intermolecular interactions of liquid dichloromethane and equilibrium properties of liquid–vapor and liquid–liquid interfaces: A molecular dynamics study, J. Chem. Phys., 110 (1999) 10113-10122.

- Six polar molecules with increasing kinetic diameter used as adsorptives
- High-resolution gas/vapour adsorption isotherms including uncertainty in the data
- Pore volumes evaluated via Gurvitsch and DR methods – inconsistencies analysed
- Low pressure isotherms show pore filling dependence on adsorptive size, shape, and polarity
- Pore filling classified into low, intermediate, and high relative pressure ranges